J Physiol (2003), **546.3**, *pp.* 777–787

DOI: 10.1113/jphysiol.2002.026328
www.jphysiol.org

Journal of Physiology

Evolution of regional performance after an acute anterior myocardial infarction in humans using magnetic resonance tagging

Frank Rademakers, Frans Van de Werf, Luc Mortelmans *, Guy Marchal † and Jan Bogaert †

*Departments of Cardiology, * Nuclear Medicine and † Radiology, University Hospitals, Leuven, Belgium*

Regional remodelling after a left ventricular myocardial infarction is the first step in a cascade that may lead to heart failure and death. To understand better the mechanisms underlying this process, it is important to study not only the evolution in local deformation parameters but also the corresponding loading conditions. Using magnetic resonance (MR) myocardial tagging, we measured the regional contribution to ejection (regional ejection fraction) and loading (systolic blood pressure × radius of curvature (mean of short and long axes)/wall thickness) in 32 regions throughout the left ventricle (LV) in patients 1 week (1W) and 3 months (3M) after a first anterior infarction. Using positron emission tomography (PET), the LV was divided into infarct, adjacent and remote regions. In the remote regions the average deformation decreased between 1W and 3M (from 59.3 ± 5.6 to 57.9 ± 6.7 %, $P < 0.05$) due to an increase in loading conditions only (from 730 ± 290 to 837 ± 299 mmHg, $P < 0.05$). In the adjacent myocardium, no change in function was observed (49.0 ± 10.8 to 49.0 ± 6.5 %, P = n.s.), although loading increased (806 ± 297 to 978 ± 287 mmHg, $P < 0.05$). In the infarct region only, an increase in deformation was seen (30.7 ± 14.2 to 37 ± 6.9 %, $P < 0.05$), together with a higher loading level (1229 ± 422 to 1466 ± 284 mmHg, $P < 0.05$), which indicates a true improvement in function. The fact that MR tagging can identify both regional deformation and loading permits us to differentiate between changes due to alterations in regional loading conditions and true changes in function. After an acute myocardial infarction (MI), an improvement can be observed in the deformation–loading relation in the adjacent and infarct regions, but the improvement is mainly in the infarct region. Using this technique, types of intervention leading to even more functional gain could be evaluated.

(Received 11 June 2002; accepted after revision 12 November 2002; first published online 20 December 2002)
Corresponding author F. Rademakers: Department of Cardiology, University Hospitals, Catholic University of Leuven, Herestraat 49, B-3000 Leuven, Belgium. Email: frank.rademakers@uz.kuleuven.ac.be

Assessment of intrinsic myocardial contractility is hampered by the load dependence of most parameters in clinical use. Left ventricular functional parameters such as stroke volume, ejection fraction (EF), fractional shortening or rate of ejection (velocity of circumferential fibre shortening (V_{cf})) are determined not only by the intrinsic myocardial contractility but also by the left ventricle (LV) pre- and afterload (Streeter *et al.* 1970; Mirsky *et al.* 1988; Legget, 1999).

After a large myocardial infarction (MI), the LV undergoes a remodelling process that involves expansion of the infarct site (Sutton & Sharpe, 2000; Giannuzzi *et al.* 2001) followed by a further decrease in LV function and enlargement of the cavity, which implicates the normal, remote regions (Kass *et al.* 1988; Kramer *et al.* 1997; Bogaert *et al.* 2000; Palojoki *et al.* 2001; Waller *et al.* 2001). This gives rise to reduced mechanical performance, electrical instability and sudden death (Gaudron *et al.* 2001). In order to understand better the mechanisms behind this remodelling process, it would be interesting to be able to judge the evolution of LV regional function in relation to the changes in local loading conditions (Dujardin *et al.* 1997; Kraitchman *et al.* 1998; Rohde *et al.* 1999; Gerber *et al.* 2000; Solomon *et al.* 2001). Magnetic resonance (MR) tagging provides this opportunity by allowing the quantification of local deformation parameters and the accurate measurement of the determinants of local loading conditions: wall thickness and curvature in two perpendicular orientations. Combining these data with systolic blood pressure gives a measure of local loading which is a relative rather than an absolute parameter, allowing comparison of loading in different regions within the same ventricle and over time in the same individual. Using the relation between local deformation and loading, a measure of myocardial performance is obtained which is more or less load independent. If this relation is applied to the infarct, adjacent and remote regions of the LV, it is possible to judge the local performance of the myocardium.

To evaluate the functional impact of a myocardial infarction over time, we therefore analysed the regional deformation–loading relations in patients after their first reperfused anterior myocardial infarction (left anterior descending coronary artery lesion without other significant coronary artery disease). Patients were evaluated in the first week after their infarction and 3 months later. Positron emission tomography (PET) imaging was used to characterize the extent of the infarct, defining the infarct, adjacent and remote regions.

METHODS

Study population

The study population consisted of 16 patients, 13 men and 3 women (mean ± S.D. age, 58 ± 10 years; range, 38–74 years), who were studied after a successful coronary reperfusion for a first transmural anterior MI. On admission, all patients presented with ST-segment elevation of ⩾ 2 mm in two or more precordial leads (V1–V6). All patients were successfully reperfused within 6 h of the onset of symptoms. Fourteen patients received intravenous thrombolytic therapy. In 10 patients an accelerated infusion of recombinant tissue-type plasminogen activator (rt-PA) was given, while four patients received 10 mg of recombinant staphylokinase over 30 min. Two other patients underwent a successful primary angioplasty. All patients developed new Q waves in the anterior leads within 24 h and had positive cardiac enzymes, diagnostic for a transmural myocardial infarction. At angiography, no significant lesions were found on other coronary arteries than the left anterior descending coronary artery. In two patients who received thrombolytic therapy, a rescue angioplasty was performed at 90 min, while in seven other patients an elective angioplasty was performed at 1 ± 2 days after the acute event.

For comparison, we also studied a control group of 31 age-matched volunteers (59.5 ± 7.1 years) without evidence of any cardiac disease (negative history, normal echocardiogram and negative bicycle stress test).

Study protocol

Approval for the study was obtained from the hospital ethics committee and written informed consent was given by all patients and volunteers. The protocols conformed to the standards set by the Declaration of Helsinki. All patients underwent coronary

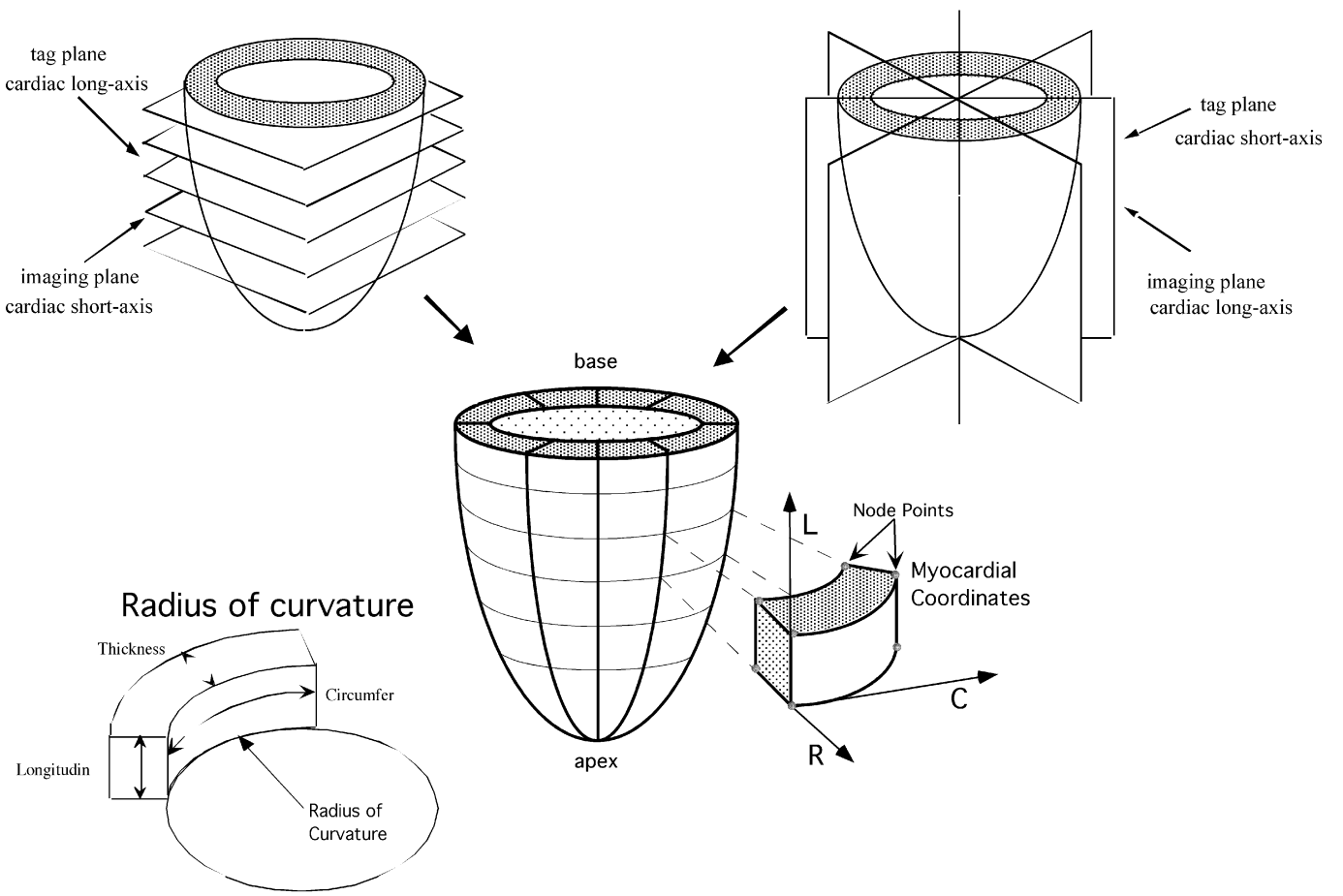

Figure 1. Regional deformation analysis with MR tagging

By means of a combination of MR tagging along the cardiac short and long axes, the LV wall is divided in 32 small cuboids. Each cuboid is defined by 4 epicardial and 4 endocardial node points. The deformation is expressed in a local cardiac coordinate system for each epicardial and endocardial node point. The axes are radial (R), circumferential (C) and longitudinal (L). In each cuboid the best circular fit to the endocardial contour is calculated in 2 circumferential and 2 radial directions. As an example, the circle (and its radius) best fitting the inferior circumferential border of a cuboid is shown.

angiography, MR tagging and PET during the first week after the acute event. All MR tagging studies were performed at 5 ± 2 days after the acute event. A second MR tagging study was performed after 3 months.

The PET study was used to define normal remote (normal flow and metabolism), adjacent (mismatch) and infarct (match decreased flow and metabolism) regions (details have been published elsewhere: Bogaert *et al.* 2000). This was preferred to a simple anatomical definition since the extent of the infarct territory in these patients with reperfused anterior infarcts was difficult to establish from the ECG or catheterization data. Functional assessment cannot be used either since it is impossible to distinguish between areas of infarction and stunning.

Matching of PET and MR results was accomplished by employing the same segmentation scheme and by using anatomical landmarks, i.e. insertion of the right ventricle and proportionality of the long axis of the left ventricle.

Magnetic resonance myocardial tagging

Principles. Magnetic resonance tagging was used to calculate myocardial deformation and loading conditions. All MR tagging studies were performed on a 1T MR unit (Magneton SP42, Siemens Erlangen, Germany), using an electrocardiographically gated and flow-compensated segmented k-space FLASH gradient-recalled echo sequence with acquisition of 3 k-lines per heart beat (repetition time 14 ms, echo time 8 ms, a variable flip angle, field of view 400 mm, matrix 180 × 256, slice thickness 8 mm). Tags were non-invasive markers placed on the myocardium by presaturating planes at end-diastole perpendicular to the subsequent imaging planes. They showed up on the images as dark lines that moved and deformed with the myocardium on which they were inscribed. Five parallel short-axis planes and four radially oriented long-axis planes crossing in the centre of the LV were defined (Fig. 1). On each of these images the crossing of the tag lines with the epi- and endocardium were identified, as well as the epi- and endocardial contours. The gravitational centre line of the LV cavity was constructed by finding the centre of the cavity on each short-axis image and fitting a line through those centre points. Images were acquired at end-diastole and end-systole in all these planes, using the short-axis planes as tagging planes for the long-axis images and vice versa. By combining the short- and long-axis information, the entire LV wall, except for the apex, could be reconstructed into 32 small cuboids for which the 3-D coordinates of the node points were known in a local cardiac coordinate system: radial, circumferential and longitudinal. For each cuboid a local deformation and loading component was calculated: the former is a composite of the deformation of that myocardial cuboid leading to local displacement of blood in the cavity and contributing to the ejection fraction (regional EF); the latter is a measure of the resistance to this deformation and to the local displacement of blood (regional loading).

Regional ejection fraction. The amount of blood ejected by each cuboid during systole is expressed by the regional EF (Fig. 2). Since the short-axis tags are radially oriented, with the crossing of the tag lines giving the LV centre, each cuboid defines an intracavitary pie-shaped volume where the endocardial surface is the base and the LV centre is the apex. At end-systole this pie-shaped volume becomes deformed due to displacement and shearing; this was taken into account in the calculations, using flat planes rather than warped surfaces to create a volume. The inward motion of the endocardium determines the change in intracavitary pie-shaped volume. The regional EF is given by:

$$\frac{\text{End-diastolic volume} - \text{end-systolic volume}}{\text{end-diastolic volume}}.$$

Regional EF, although defined as an intracavitary parameter, thus represents the composite of the deformation of the adjacent myocardial cuboid. It incorporates radial thickening, longitudinal shortening and circumferential shortening, culminating in an inward motion of the endocardium and displacement of blood by the deforming cuboid.

Myocardial wall thickness, circumferential and longitudinal radius of curvature. True myocardial wall thickness was obtained using 3-D information, by adjusting tag length for wall curvature in the longitudinal direction. The circumferential and longitudinal radii of curvature were calculated in each cuboid using the calculated chord and measured arch lengths fitting a model (Fig. 1). This yielded a radius of curvature at each border of a cuboid: 4 in the circumferential direction and 4 in the longitudinal direction (2 each at the epicardium and at the endocardium). A small radius of curvature denotes a curved surface, while a large radius of curvature is representative of a flat surface. In this study the radii of curvature at the endocardium in both the longitudinal and circumferential direction were used.

Regional loading conditions. Highly complex formulas have been used to calculate myocardial wall stress (DeAnda *et al.* 1998; Solomon *et al.* 1998; Taniguchi *et al.* 1998). They all rely on assumptions regarding myocardial material properties, shape and configuration of the ventricle. We used very simple parameters, known to be related to wall stress, assumed a simple linear direct relation and combined them in one value (Grossman *et al.* 1977; Fujita *et al.* 1993; Balzer *et al.* 1999): regional load = [systolic blood pressure × (mean radius of curvature in short and long axis)]/3-D wall thickness. An average of the short- and long-axis radii of curvature was used, although the relative contribution of these two measurements to load probably differs; since no data are available, however, to determine the exact ratio, a simple average (50 % weight) was used. This calculated value of load certainly does not quantify absolute wall stress but is only intended to determine relative differences of local loading conditions between individuals (i.e. systolic blood pressure) and within the ventricle (i.e. regional wall thickness and radii of curvature). The term 'load' will be used in this paper to denote this regional parameter.

To relate deformation to loading conditions, regional EF was regressed *versus* regional loading.

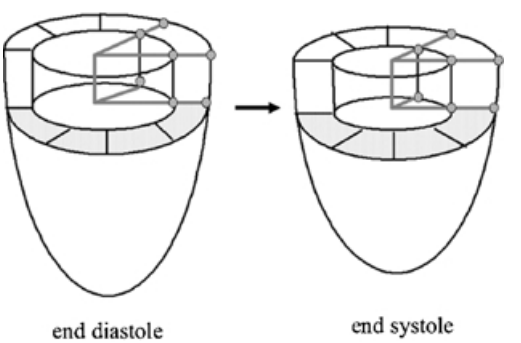

Figure 2. Regional ejection fraction

The delineation of a pie-shaped intracavitary volume by adjacent tag lines, crossing in the centre of the cavity, is shown at end-diastole and end-systole.

Table 1. Radius of curvature in the short axis

RC SA	Infarct		Adjacent		Remote	
location	1 week	3 month	1 week	3 month	1 week	3 month
1	1.54	1.55	1.65	1.70	1.62	1.83
2	1.51	1.57	1.56	1.67	1.67	1.78
3	0.93	1.11	0.99	1.06	1.52	1.38
4	0.50	1.04	0.47	0.66	0.79	0.91
5	—	—	0.38	0.71	0.71	0.84
6	0.63	1.11	0.93	1.02	1.13	1.23
7	1.71	1.59	1.59	1.75	1.69	1.69
8	1.74	1.63	1.74	2.13	1.62	2.10

Radius of curvature (cm) in the short axis (RC SA) at 8 locations around the circumference of the ventricle (averaged from base to apex), in the infarct, adjacent and remote zones, at the 1 week and 3 month studies.

Table 2. Radius of curvature in the long axis

RC LA	Infarct		Adjacent		Remote	
location	1 week	3 month	1 week	3 month	1 week	3 month
1	6.65	6.47	8.33	7.63	8.07	8.06
2	5.73	5.70	7.98	7.57	7.81	7.55
3	4.48	4.64	5.98	5.90	7.35	7.26
4	1.90	1.99	5.42	4.99	6.51	6.32
5	—	—	4.17	4.70	6.41	6.09
6	3.55	3.92	5.84	5.55	7.03	7.14
7	5.48	5.41	7.00	7.02	7.59	7.39
8	6.44	6.28	7.84	7.70	7.77	7.58

Radius of curvature (cm) in the long axis (RC LA) at 8 locations around the circumference of the ventricle (averaged from base to apex), in the infarct, adjacent and remote zones, at the 1 week and 3 month studies.

Statistical analysis

All data are expressed as means ± S.D. Differences between the two evaluations over time in the same patients, were evaluated using the repeated measures ANOVA; to find significant differences between regions in the infarct patients an ANOVA was used; *post hoc* testing was performed using the Scheffé test; a P value < 0.05 was considered significant. To relate deformation to loading, we used simple linear regression analysis. The regression lines of a group of normals with a confidence interval of 2 S.D. are shown as reference. For the infarct patients a mean deformation and loading level was also calculated for each region (remote, adjacent, infarcted) at 1 week (1W) and 3 months (3M) as well as the individual regression lines. These regression lines were calculated for each region in each individual and subsequently the slopes, intercepts and correlation coefficients were averaged for all regions in the different patients. For graphical display, the averaged regression curves are shown together with the averaged data points per region for all individuals.

RESULTS

Results of regional strains (Bogaert *et al.* 1999), wall thickness and radii of curvature (Bogaert *et al.* 2000) have been published previously. Key results and average values are repeated here.

Haemodynamic and global changes

In normals, heart rate was 73 ± 11 beats min^{-1} and blood pressure was 127 ± 10/78 ± 6 mmHg. In the infarct patients there were no significant differences in heart rate or blood pressure between the 1W and 3M studies (70 ± 12 beats min^{-1} and 141 ± 13/85 ± 9 mmHg for the 1W study *versus* 68 ± 10 beats min^{-1} and 145 ± 14/84 ± 7 mmHg for the 3 month study; P = n.s.). Global ejection fraction was 63 ± 5 % in the normal individuals; in the infarct patients it increased from 42 ± 12 to 49 ± 8 %, while end-diastolic volume increased from 105 ± 32 to 115 ± 29 ml and end-systolic volume decreased from 63 ± 25 to 59 ± 19 ml (all $P < 0.01$). Average wall thickness was 0.96 ± 0.15 cm in normals; in the infarct patients wall thicknesses at 1 week for the remote, adjacent and infarct regions were 1.08 ± 0.19, 1.13 ± 0.19 and 1.13 ± 0.19 cm, respectively; at 3 months the results were 1.02 ± 0.20, 1.06 ± 0.19 and 1.07 ± 0.20 cm, respectively (all decreased significantly from 1 week to 3 months). The higher wall thickness in the infarct and adjacent zones, compared to the remote zone could be related to oedema in the reperfused myocardium. Wall thinning was observed in the infarct and adjacent regions over time, but also in the remote area (all $P < 0.05$). The changes in radii of curvature at the endocardium in the short and long axes around the circumference of the ventricle are shown in Tables 1 and 2. Since the size and location of the infarct, adjacent and remote regions differed from patient to patient, a variable number of data points was available for each location around the ventricle (averaged from base to apex) in each of these regions. For the infarct region no data were present at location 5 (inferior) while a limited number of data were present in locations 4 and 6 of the infarct region and in locations 1–2 (septal) and 7–8 (anterior) for the remote zone. Due to this inter-individual variation, no significant difference could be observed between 1 week and 3 months; a trend toward an increase in the short-axis radius and a decrease in the long-axis radius can be seen (this corresponds to an evolution of an ellipsoidal to a more spherical ventricle).

Average load and regional EF levels

In the normal age-matched individuals, mean regional EF was 64.7 ± 5.8 % and mean loading was 877 ± 254 mmHg. In the infarct patients, mean regional EF and loading in the 1W study were 46.4 ± 11.9 % ($P < 0.05$ *versus* normals) and 922 ± 221 mmHg (P = n.s. *versus* normals), respectively. Mean regional EF and loading in each region were 59.3 ± 5.6 % and 730 ± 290 mmHg, respectively, in the remote region; 49.0 ± 10.8 % and 806 ± 297 mmHg, respectively, in the adjacent region; 30.7 ± 14.2 % and 1229 ± 422 mmHg, respectively, in the infarcted region. In the 3 months study overall regional EF and loading were 48.1 ± 8.4 % ($P < 0.05$ *versus* normals) and 1094 ± 271 mmHg ($P < 0.05$ *versus* normals), respectively, while mean values for each region were 57.9 ± 6.7 % and

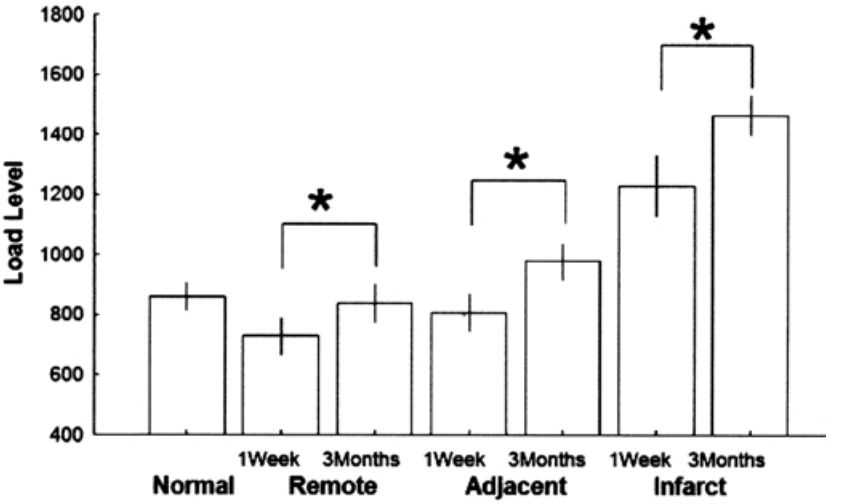

Figure 3. Average load values

The average load values and standard deviation are shown in the controls (Normal) and in the infarct patients (Infarct, Adjacent and Remote regions for the 1W and 3 M studies). * $P < 0.01$.

837 ± 299 mmHg, respectively, in the remote region; 49.0 ± 6.5 % and 978 ± 287 mmHg, respectively, in the adjacent region; 37 ± 6.9 % and 1466 ± 284 mmHg, respectively, in the infarcted region. Between 1W and 3M all changes in loading were significant (Fig. 3), while only the changes in the remote and infarct regions were significant for regional EF.

Regression of deformation *versus* loading

The simple linear regression in age-matched normals resulted in a very tight relation between regional EF and loading: regional EF = 79 – 0.019 × regional load; $r^2 = 0.762$. The results for the infarct patients were more scattered but still showed a significant relation in the different regions: at 1 week: in the remote zone: regional EF = 68 – 0.011 × regional load; $r^2 = 0.349$; in the adjacent zone: regional EF = 70 – 0.026 × regional load; $r^2 = 0.513$; in the infarct zone: regional EF = 64 – 0.027 × regional load; $r^2 = 0.651$; at 3 months: in the remote zone: regional EF = 73 – 0.018 × regional load; $r^2 = 0.665$; in the adjacent zone: regional EF = 57 – 0.009 × regional load; $r^2 = 0.142$; in the infarct zone: regional EF = 57 – 0.013 × regional load; $r^2 = 0.308$; all results $P < 0.001$. Graphical results for mean deformation and loading in the infarct patients, compared to the regression curve of the normals is shown in Fig. 4, while Fig. 5 shows the regression lines for the different territories of the infarct patients at 1 week and 3 months (significant difference for the slope coefficient for the infarct and adjacent zones).

The up-rotation of the deformation–load relation in the infarct and adjacent territories corresponds to a higher deformation at a similar load level and can be interpreted as an increase in intrinsic myocardial performance. In the remote zone no significant downward rotation was observed, corresponding to a maintained myocardial performance in this region.

The large standard deviations are due in part to inter-individual differences but also to a large extent to the regional variation within the ventricle. This is demonstrated in Figs 6 and 7, showing regional EF (panel *A* in Figs 6 and 7) and regional load (panel *B* in Figs 6 and 7) variation around the circumference of the ventricle and along the long axis of the ventricle, respectively, for the infarct, adjacent and remote territories. Values are averaged base to apex for the circumferential data and around the circumference for the longitudinal data. Especially for the infarct and adjacent regions, the number of actual segments, contributing to these averages, can be very small (no data for location 5 in the infarct region (Fig. 6); few data in locations 4 and 6). No significant differences in load or regional EF could therefore be observed, but the consistent inverse regional relation between load and regional EF can be seen.

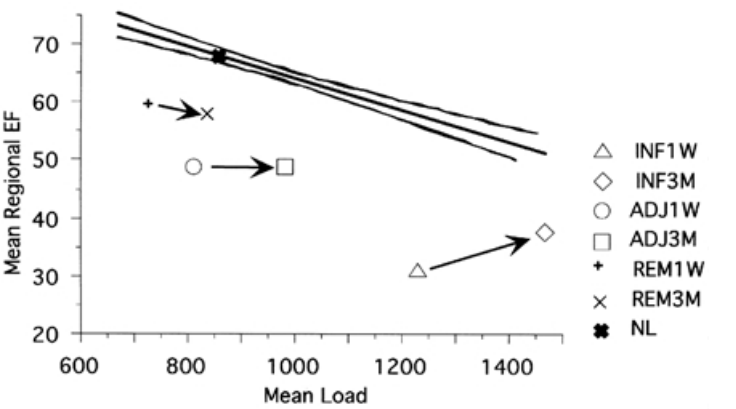

Figure 4. Relation between mean regional ejection fraction and load

The relation between average regional ejection fraction and average load is shown for the different regions and for the 1W and 3M studies. For reference the normal relation and regression line with 2 S.D. confidence lines are also depicted.

In the infarct patients, the larger variability is due to the incorporation of remote, adjacent and infarct regions in the averages; in the normals, the variation is smaller but still present and can only be accounted for by the differences in regional wall thickness and curvature. Beside the regional inverse relation between regional EF and loading, the higher loading levels in the antero-septal region and near the base (also in the normal individuals) can be appreciated.

DISCUSSION

Radial MR tagging allows the calculation of regional deformation and loading components, which represent the average contribution of that part of the myocardial wall to ejection and the resistance to ejection in that same region, respectively. Although these parameters do not represent wall strain and stress, they are a composite of the resultant of wall deformation and an indicator of the corresponding load; the validity of this approach can be judged from the tight relation between the regional load and deformation components in normal individuals, where the variation in the load component explains 76 % of the variation in deformation. This is a relatively high value for a biological system, also taking into account the variation introduced by the imaging technique itself and the contouring of the images from which the calculations are made. The strength of the relation is less in the infarct patients, reflecting the more inhomogeneous behaviour and other factors influencing the relationship (degree of transmurality of the infarct, tethering by adjacent zones, medication, etc.).

In the infarct patients, several observations can be made. Although all the patients were treated state-of-the-art with early revascularization, beta blockers and ACE inhibitors, load levels increased in all regions between the 1W and 3M examinations. This led to a decrease in regional EF values in the remote regions; since the change occurs on a parallel but inferior course to the line of the normals (Fig. 4) and since the regression coefficients in Fig. 5 are similar, this can be interpreted as an absence of change in intrinsic performance over time but as a change caused by the increased loading conditions in this region. The reasons for the lower performance in the remote, normally perfused regions (lower deformation values for similar

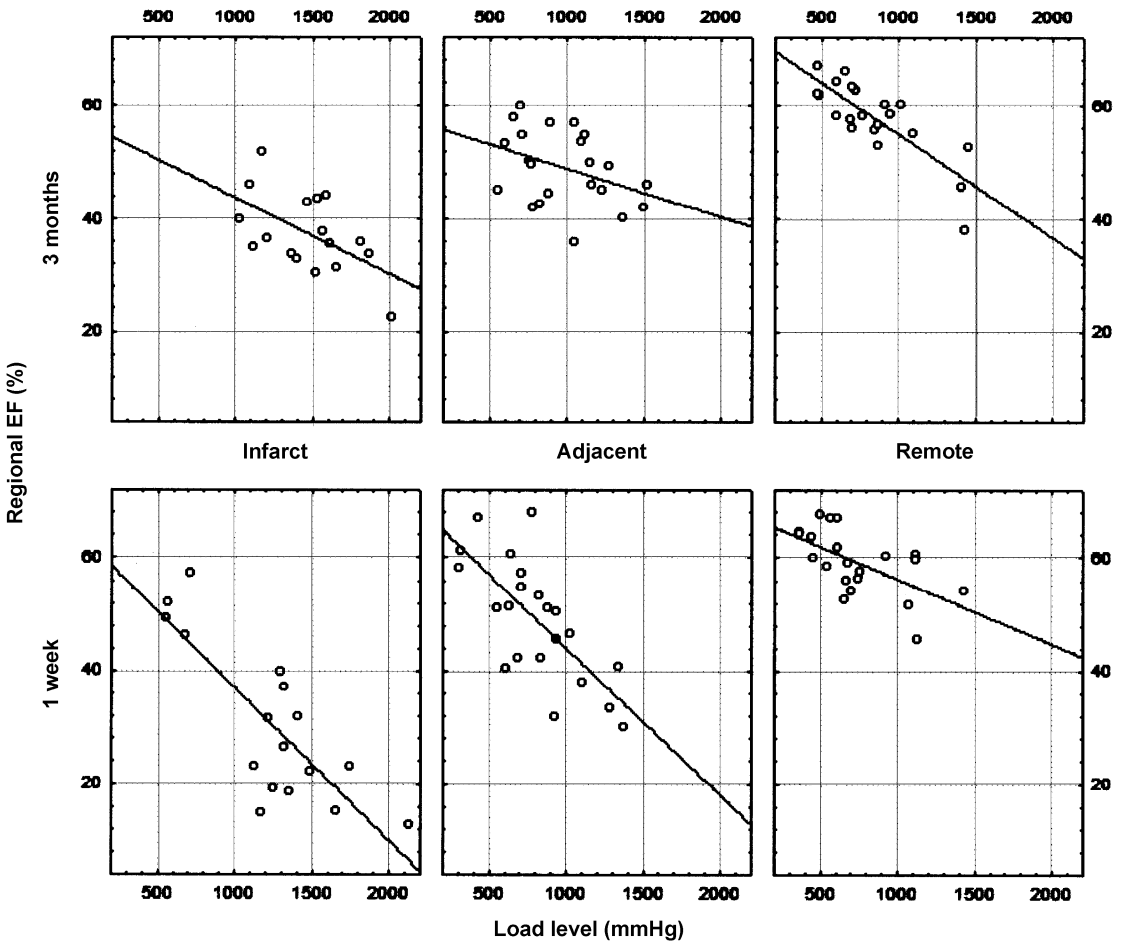

Figure 5. Regression between regional ejection fraction and load

The different regression lines between regional ejection fraction and load are shown in the different regions for the 1W and 3M studies in the infarct patients.

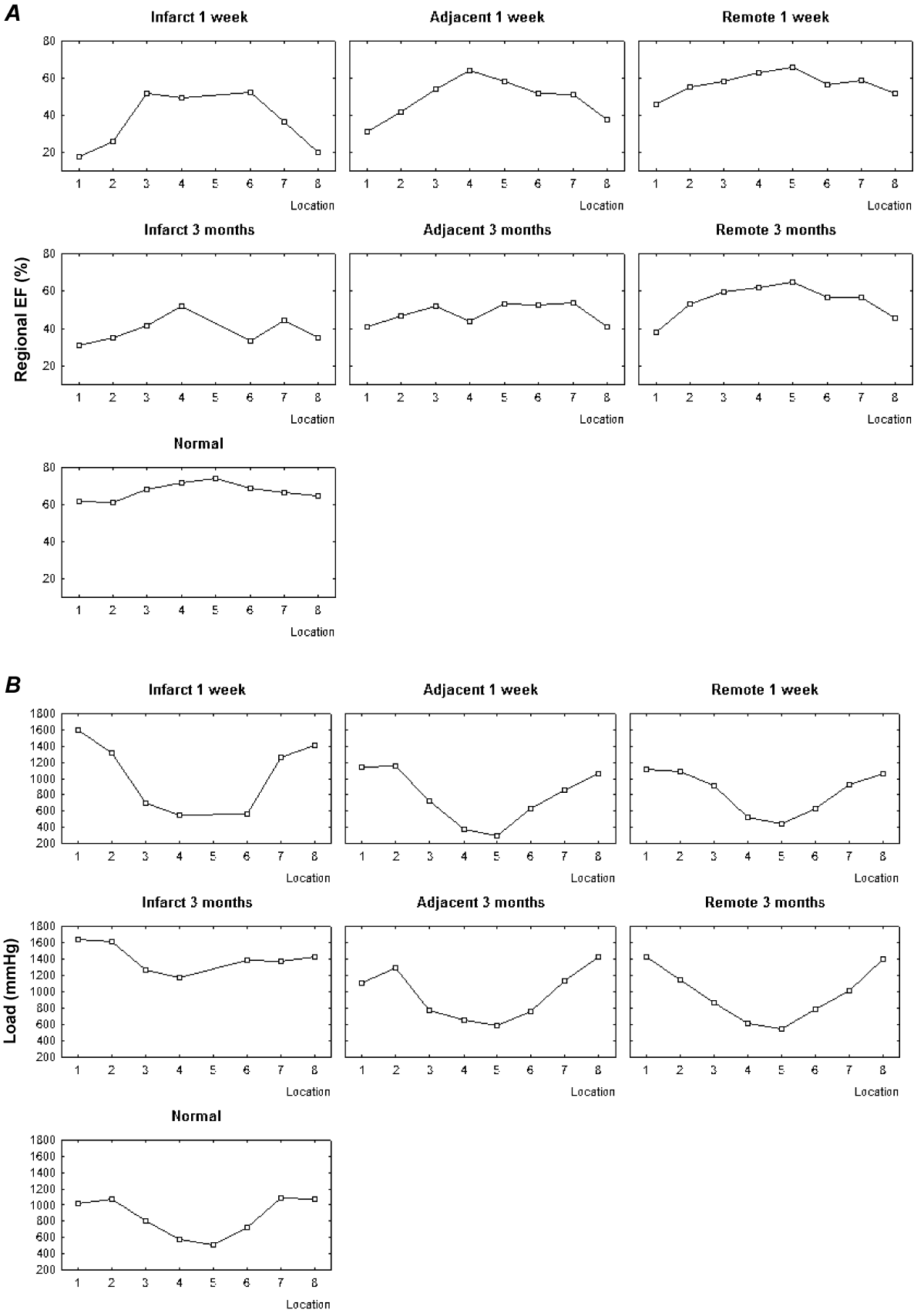

Figure 6. Distribution of regional EF (*A*) and load (*B*) around the circumference of the ventricle

Data shown for normals and infarct patients in the different regions (remote, adjacent, infarcted) at 1 week and 3 months. Eight locations around the circumference are shown: location 1–3 corresponds to interventricular septum, 4–5 to inferior wall, 6 to lateral wall, 7–8 to anterior wall.

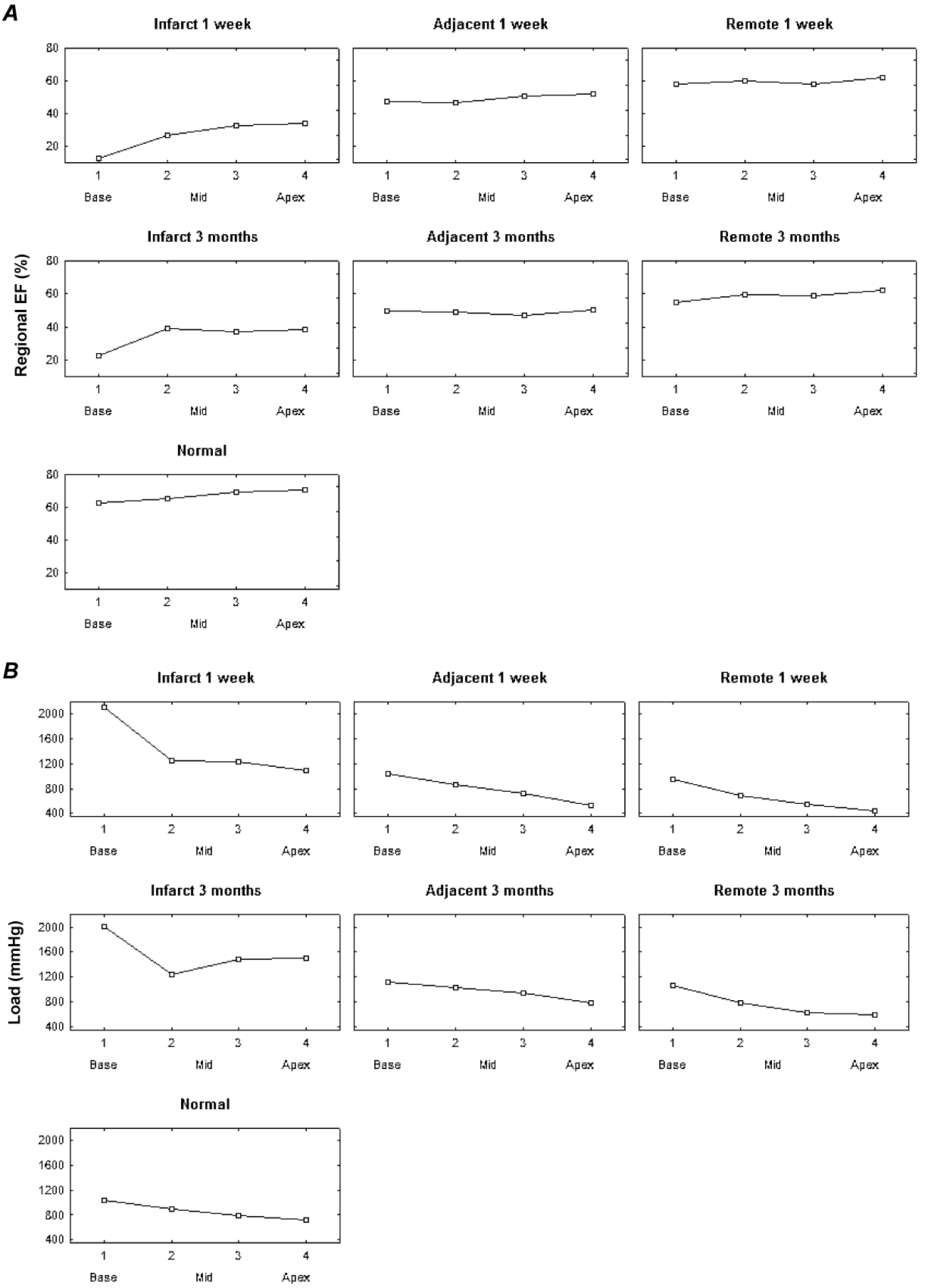

Figure 7. Distribution of regional EF (*A*) and load (*B*) along the long axis of the ventricle

Data shown for normals and infarct patients in the different regions (remote, adjacent, infarcted) at 1 week and 3 months. Four levels from base to apex are shown: 1 base, 4 apex.

loading levels in comparison to controls) remain to be established, but do not seem to be attributable to an absolute increase of the average load levels over time; on the contrary, average load levels are slightly lower than in control individuals. Further analysis, looking for separate loading levels in the circumferential and longitudinal directions, will have to be performed, since it was shown that longitudinal deformation was most affected in the remote zone (Bogaert *et al.* 2000). Possible causes of decreased performance beside changes in load levels could relate to decreased intrinsic contractility, secondary to perfusion abnormalities at the microcirculatory level, possibly induced by overstimulation by catecholamines, inflammatory changes, altered regional neuro-adrenergic drive, function–perfusion mismatch (compensatory hypertrophy without adequate capillary growth), etc. Some of these mechanisms are more likely to be at work in the infarct and adjacent regions, but they could also influence the remote zones.

The alterations in the adjacent and infarct regions, on the other hand, have a different course from those in the remote area. In the adjacent myocardium, no change in regional EF was observed, although the loading levels significantly increased over the observation period. This corresponds to a regression line which rotates upward. This could be explained by an increase in intrinsic performance which does not translate into a larger deformation, due to the concomitant increase in the loading conditions. Finally, the infarct region shows a significant increase in regional EF. The fact that this occurs in view of increasing loading levels again implies a true enhancement of function (up-rotation of regression lines), due to recovery of the subepicardial myocardial layers, as has previously been shown (Bogaert *et al.* 1999). This recovery over 3 months can be interpreted as the recovery of viable but stunned myocardium in the subepicardial and bordering regions of the infarct. The subepicardial rim of viable myocardium in the infarct region can be seen in much the same way as the viable myocardium neighbouring the infarct. Both are in the territory of the infarct-related occluded artery and suffer from stunning and reperfusion injury. Only by looking at the relation between deformation and loading, could this similarity in behaviour be identified, since deformation itself was unchanged in the adjacent myocardium. This can be explained by the 'tethering' between infarcted and viable myocardium: the increased load on the expanded, partially fibrosed infarct region pulls sideways on the adjacent segments, increases their load and causes an unaltered deformation level, although a recovery in intrinsic function is present. Similarly, the remote regions will 'feel', but to a smaller degree, the increased pull from the infarcted zone. This leads to the concept of muscle interaction or 'tethering' not only due to direct, local connections, but also at a distance, since muscle fibres are a continuum, turning on themselves in a figure-of-eight configuration. In how far this could also influence the sequence of muscle innervation, due to slowing or acceleration of the electric impulse in the fibrotic area remains to be established.

Although not proven, it seems likely that such interactions at a distance and global shape and configuration changes of the ventricle can also play an important role in influencing regional, mechanical performance in the remote, so-called normal myocardium. Surgical and pharmacological interventions should take this into account and be tested not only for their influence on global parameters, i.e. ejection fraction, end-diastolic volume, but also on shape, regional performance and interaction.

One can speculate that the functional benefit of the recovery of function in the infarct and adjacent zones could be enhanced by better control of the loading conditions. The global increase in load is amplified by the enlargement of the ventricle which affects the infarct and adjacent myocardium more than the remote zones (larger increase in loading values): infarct remodelling.

The up-rotation of the regression lines not only indicates a better performance at a given load level but also can be interpreted as a decrease in load dependence of the myocardium: the regression lines do not just simply shift upwards but they rotate and the relation becomes flatter: less variation in deformation exists for a given change in load levels. The cause and physio-pathological implications of this finding warrant further study.

While it is presently impossible to calculate these parameters routinely for every patient with the current state of automated contouring, the deformation–loading relation is very well suited for evaluation of interventions (pharmacological: Wei *et al.* 2000; Aikawa *et al.* 2001; surgical: Athanasuleas *et al.* 1998, 2001; or other: Cleutjens *et al.* 1999; Kanamasa *et al.* 2000; Yousef *et al.* 2000) on the remodelling process. If computer-aided contouring or other tagging analyses become more robust, these parameters could also be very easily computed for individual patients to guide their specific therapy (Jain *et al.* 2001). It has to be noted, however, that at present only radial tagging, and not spacial modulation of magnetization (SPAMM) or line-tagging, provides an easy measurement of regional ejection fraction and radii of curvature. Further study could define other calculations of loading levels which could be used to relate to radial, circumferential and longitudinal strain and eventually fibre strain, which would further enhance our understanding of the pathophysiology behind the remodelling process after a myocardial infarction.

Limitations

In this study we did not quantify absolute loading levels, but our data, based only on measurable parameters such as

wall thickness and radii of curvature, provide relative measures of loading levels. We also used systolic blood pressure rather than end-systolic blood pressure for the load calculations. Since the intracavitary pressure is similar throughout the LV, this parameter has no influence on the relation between regional EF and load in one individual.

We could not avoid including tissues with different characteristics (infarcted, stunned, remote) in one region of interest (32 regions of tagging and PET examinations). This is probably another reason why the relation between load and deformation was less tight in the infarct patients than in the normals. It is also possible that the infarct zone itself is inhomogeneous in character.

Only a limited number of patients were included in the study, mainly due to the complex nature of the investigations (MR and PET); future studies with more patients should enable us to investigate the impact of pharmacologic al or other interventions.

Conclusion

MR radial tagging provides a method of quantifying the regional contribution to ejection and regional loading conditions, which can be used to interpret better changes in intrinsic performance of the myocardium. In patients after an anterior myocardial infarction, this approach shows that the decrease in function over time in the remote zone is due to an increase in load level only, while the unchanged deformation in the adjacent zone could actually represent an increase in performance, which is also present in the infarct region.

REFERENCES

Aikawa Y, Rohde L, Plehn J, Greaves SC, Menapace F, Arnold MO, Rouleau JL, Pfeffer MA, Lee RT & Solomon SD (2001). Regional wall stress predicts ventricular remodeling after anteroseptal myocardial infarction in the healing and early afterload reducing trial (heart): An echocardiography-based structural analysis. *Am Heart J* **141**, 234–242.

Athanasuleas CL, Stanley Aw Jr & Buckberg GD (1998). Restoration of contractile function in the enlarged left ventricle by exclusion of remodeled akinetic anterior segment: Surgical strategy, myocardial protection, and angiographic results. *J Card Surg* **13**, 418–428.

Athanasuleas CL, Stanley Aw Jr, Buckberg GD, Dor V, Didonato M & Blackstone EH (2001). Surgical anterior ventricular endocardial restoration (saver) in the dilated remodeled ventricle after anterior myocardial infarction. Restore group. Reconstructive endoventricular surgery, returning torsion original radius elliptical shape to the lv. *J Am Coll Cardiol* **37**, 1199–1209.

Balzer P, Furber A, Delepine S, Rouleau F, Lethimonnier F, Morel O, Tadei A, Jallet P, Geslin P & Le Jeune JJ (1999). Regional assessment of wall curvature and wall stress in left ventricle with magnetic resonance imaging. *Am J Physiol* **277**, H901–910.

Bogaert J, Bosmans H, Maes A, Suetens P, Marchal G & Rademakers FE (2000). Remote myocardial dysfunction after acute anterior myocardial infarction: Impact of left ventricular shape on regional function: A magnetic resonance myocardial tagging study. *J Am Coll Cardiol* **35**, 1525–1534.

Bogaert J, Maes A, Van de Werf F, Bosmans H, Herregods M, Nuyts J, Desmet W, Mortelmans L, Marchal G & Rademakers FE (1999). Functional recovery of subepicardial myocardial tissue in transmural myocardial infarction after successful reperfusion. *Circulation* **99**, 36–43.

Cleutjens JP, Blankesteijn WM, Daemen M J & Smits JF (1999). The infarcted myocardium: Simply dead tissue, or a lively target for therapeutic interventions. *Cardiovasc Res* **44**, 232–241.

DeAnda A Jr, Komeda M, Moon MR, Green GR, Bolger AF, Nikolic SD, Daughters GT 2nd & Miller DC (1998). Estimation of regional left ventricular wall stresses in intact canine hearts. *Am J Physiol* **275**, H1879–1885.

Dujardin KS, Enriquez-Sarano M, Rossi A, Bailey KR & Seward JB (1997). Echocardiographic assessment of left ventricular remodeling: Are left ventricular diameters suitable tools? *J Am Coll Cardiol* **30**, 1534–1541.

Fujita N, Duerinckx AJ & Higgins CB (1993). Variation in left ventricular regional wall stress with cine magnetic resonance imaging: Normal subjects *versus* dilated cardiomyopathy. *Am Heart J* **125**, 1337–1345.

Gaudron P, Kugler I, Hu K, Bauer W, Eilles C & Ertl G (2001). Time course of cardiac structural, functional and electrical changes in asymptomatic patients after myocardial infarction: Their interrelation and prognostic impact. *J Am Coll Cardiol* **38**, 33–40.

Gerber BL, Rochitte CE, Melin JA, McVeigh ER, Bluemke DA, Wu KC, Becker LC & Lima JA (2000). Microvascular obstruction and left ventricular remodeling early after acute myocardial infarction. *Circulation* **101**, 2734–2741.

Giannuzzi P, Temporelli PL, Bosimini E, Gentile F, Lucci D, Maggioni AP, Tavazzi L, Badano L, Stoian I, Piazza R, Heyman I, Levantesi G, Cervesato E, Geraci E & Nicolosi GL (2001). Heterogeneity of left ventricular remodeling after acute myocardial infarction: Results of the gruppo italiano per lo studio della sopravvivenza nell'infarto miocardico-3 echo substudy. *Am Heart J* **141**, 131–138.

Grossman W, Braunwald E, Mann T, McLaurin L & Green L (1977). Contractile state of the left ventricle in man as evaluated from end-systolic pressure-volume relations. *Circulation* **56**, 845–852.

Jain M, Dersimonian H, Brenner DA, Ngoy S, Teller P, Edge AS, Zawadzka A, Wetzel K, Sawyer DB, Colucci WS, Apstein CS & Liao R (2001). Cell therapy attenuates deleterious ventricular remodeling and improves cardiac performance after myocardial infarction. *Circulation* **103**, 1920–1927.

Kanamasa K, Ishikawa K, Ogawa I & Nakabayashi T (2000). Prevention of left ventricular remodeling by percutaneous transluminal coronary angioplasty performed 24 h after the onset of acute myocardial infarction. *J Thromb Thrombolysis* **9**, 47–51.

Kass DA, Maughan WL, Ciuffo A, Graves W, Healy B & Weisfeldt ML (1988). Disproportionate epicardial dilation after transmural infarction of the canine left ventricle: Acute and chronic differences. *J Am Coll Cardiol* **11**, 177–185.

Kraitchman DL, Young, AA, Bloomgarden DC, Fayad ZA, Dougherty L, Ferrari VA, Boston RC & Axel L (1998). Integrated MRI assessment of regional function and perfusion in canine myocardial infarction. *Magn Reson Med* **40**, 311–326.

Kramer CM, Rogers WJ, Theobald TM, Power TP, Geskin G & Reichek N (1997). Dissociation between changes in intramyocardial function and left ventricular volumes in the eight weeks after first anterior myocardial infarction. *J Am Coll Cardiol* **30**, 1625–1632.

Legget M (1999). Usefulness of parameters of left ventricular wall stress and systolic function in the evaluation of patients with aortic stenosis. *Echocardiography* **16**, 701–710.

Mirsky I, Corin WJ, Murakami T, Grimm J, Hess OM & Krayenbuehl HP (1988). Correction for preload in assessment of myocardial contractility in aortic and mitral valve disease: Application of the concept of systolic myocardial stiffness. *Circulation* **78**, 68–80.

Palojoki E, Saraste A, Eriksson A, Pulkki K, Kallajoki M, Voipio-Pulkki LMV & Tikkanen I (2001). Cardiomyocyte apoptosis and ventricular remodeling after myocardial infarction in rats. *Am J Physiol Heart Circ Physiol* **280**, H2726–2731.

Rohde LE, Aikawa M, Cheng GC, Sukhova G, Solomon SD, Libby P, Pfeffer J, Pfeffer MA & Lee RT (1999). Echocardiography-derived left ventricular end-systolic regional wall stress and matrix remodeling after experimental myocardial infarction. *J Am Coll Cardiol* **33**, 835–842.

Solomon SD, Aikawa Y, Martini MS, Rosario L, Makker G, Gerson D, Greaves S & Lee RT (1998). Assessment of regional left ventricular wall stress after myocardial infarction by echocardiography-based structural analysis. *J Am Soc Echocardiogr* **11**, 938–947.

Solomon SD, Glynn RJ, Greaves S, Ajani U, Rouleau JL, Menapace F, Arnold JM, Hennekens C & Pfeffer MA (2001). Recovery of ventricular function after myocardial infarction in the reperfusion era: The healing and early afterload reducing therapy study. *Ann Intern Med* **134**, 451–458.

Streeter DD, Vaishnav RN, Patel DJ, Spotnitz HM, Ross JJ & Sonnenblick EH (1970). Stress distribution in the normal canine left ventricle during diastole and systole. *Biophys J* **10**, 345–363.

Sutton MG & Sharpe N (2000). Left ventricular remodeling after myocardial infarction: Pathophysiology and therapy. *Circulation* **101**, 2981–2988.

Taniguchi K, Sakurai M, Takahashi T, Imagawa H, Mitsuno M, Nakano S, Kawashima Y & Matsuda H (1998). Postinfarction left-ventricular aneurysm: Regional stress, function, and remodeling after aneurysmectomy. *Thorac Cardiovasc Surg* **46**, 253–259.

Waller C, Hiller KH, Kahler E, Hu K, Nahrendorf M, Voll S, Haase A, Ertl G & Bauer WR (2001). Serial magnetic resonance imaging of microvascular remodeling in the infarcted rat heart. *Circulation* **103**, 1564–1569.

Wei S, Chow LT & Sanderson JE (2000). Effect of carvedilol in comparison with metoprolol on myocardial collagen postinfarction. *J Am Coll Cardiol* **36**, 276–281.

Yousef ZR, Redwood SR & Marber MS (2000). Postinfarction left ventricular remodeling: A pathophysiological and therapeutic review. *Cardiovasc Drugs Ther* **14**, 243–252.

Acknowledgements

The study has been supported in part by grant no. G3132.94 from the Fonds voor Wetenschappelijk Onderzoek (FWO).